International Journal of Aeronautics and Astronautics
https://dergipark.org.tr/en/pub/ijaa

2025, VOL:6, ISS:1, 1-12 e-ISSN: 2757-6574

Research Article / Araştırma Makalesi

Aerodynamic insights from peregrine falcon flight using CFD: Applications in aircraft engineering / Alaca doğanının uçuş dinamiklerinden CFD ile elde edilen aerodinamik bulgular: Havacılık mühendisliğinde uygulamalar

Cihan Bayındırlı*

[1] *Program of Automotive Technology, Nigde Vocational School of Technical Sciences, Nigde Omer Halisdemir University, Nigde, Türkiye*

Received	Revised	Accepted
November 12, 2024	February 17, 2025	March 3, 2025

Keywords
Aerodynamic,
Aircraft,
CAD design,
C_D coefficient,
Drag force,

Anahtar Kelimeler
Aerodinamik,
Uçak,
CAD tasarımı,
C_D katsayısı,
Sürükleme kuvveti,

ABSTRACT

In this study, the aerodynamic characteristics of the peregrine falcon were analyzed using the Computational Fluid Dynamics (CFD) method. The falcon model scaled 1:1, was designed in SolidWorks® for both gliding and diving scenarios. Ansys Fluent® was employed to determine the drag and lift coefficients of the bird model. Numerical analyses were conducted at four different flow rates with Reynolds numbers ranging from 753205 to 3012821. The average drag coefficient (C_D) during diving was 0.00933, while the lift coefficient (C_L) was 0.00428, resulting in a C_D/C_L ratio 2.18. The average drag coefficient was for gliding 0.0227, and the lift coefficient was 0.0165, with a reduced C_D/C_L ratio of 1.38. Additionally, the flow structure around the bird model was examined to identify regions where pressure-induced drag forces were significant. The study discusses potential applications for aircraft and passive flow control components inspired by the peregrine falcon's superior aerodynamic features.

ÖZET

Bu çalışmada, alaca doğanın aerodinamik özellikleri Hesaplamalı Akışkanlar Dinamiği (HAD) yöntemi kullanılarak analiz edilmiştir. 1:1 ölçeklendirilmiş doğan modeli, hem süzülme hem de dalış senaryoları için SolidWorks®'te tasarlanmıştır. Kuş modelinin sürükleme ve kaldırma katsayılarını belirlemek için Ansys Fluent® program kullanılmıştır. Sayısal analizler, 753205 ile 3012821 arasında değişen Reynolds sayılarına sahip dört farklı akış hızında gerçekleştirilmiştir. Dalış sırasında ortalama sürüklenme katsayısı (C_D) 0,00933 olurken, kaldırma katsayısı (C_L) 0,00428 olarak belirlenmiş ve bunun sonucunda C_D/C_L oranı 2,18 olmuştur. Süzülme sırasında ortalama sürüklenme katsayısı 0,0227 ve kaldırma katsayısı 0,0165 olarak bulunmuş, C_D/C_L oranı ise 1,38'e düşmüştür. Ayrıca, basınç kaynaklı sürüklenme kuvvetlerinin önemli olduğu bölgeleri belirlemek için kuş modeli etrafındaki akış yapısı incelenmiştir. Çalışma, doğan kuşun üstün aerodinamik özelliklerinden esinlenerek uçak ve pasif akış kontrol bileşenleri için potansiyel uygulamaları tartışmaktadır.

* Corresponding author, e-mail: cbayindirli@ohu.edu.tr

Citation: *Bayındırlı, C. 2025 Aerodynamic insights from peregrine falcon flight using CFD: Applications in aircraft engineering, International Journal of Aeronautics and Astronautics 6(1), 1-12.*

Nomenclature

$\mathbf{F_D}$	Drag force, N	$\boldsymbol{\nu}$	Kinematic viscosity, m^2/s
$\mathbf{C_D}$	Drag coefficient	$\boldsymbol{\rho}$	Density, kg/m^3
$\mathbf{C_L}$	Lift coefficient	**CFD**	Computational fluid dynamics
©	Trademark	**CAD**	Computer-aided design
Re	Reynolds number		

1. Introduction

The flying speed of birds varies depending on their species and anatomical structure. Factors that affect flying speeds include wing shape, muscle strength, and aerodynamic design. Some bird species can reach extremely high speeds while hunting or escaping from predators. For example, falcons and falcons can chase prey at speeds of up to 300-320 kilometers per hour. This speed is accompanied by their sharp eyes and fast maneuvering abilities. The peregrine falcon (Falco peregrinus) is one of the fastest birds in the world. It reaches speeds of up to 150 km/h during horizontal flight [1] and even reaches speeds of over 320 km/h when nose-diving to attack bird prey [2]. Almost all bird species can change the shape of their wings and thus their aerodynamic properties a concept known as the "transforming wing" [3-5]. While diving, peregrines also change the shape of their wings; as they accelerate and move them increasingly closer to their bodies. Their various body shapes can be described as the classic diamond shape of the wings followed by the tight vertical fold with the dimple-like profile of the forewing parts [6-7]. Peregrines are not only extremely fast flyers, but they also have remarkable maneuverability at high speeds. For example, during courtship behavior, they often change flight paths at the end of the dive, i.e. from a vertical dive to a steep climb. This suggests that peregrines are exposed to high mechanical loads [8]. Among biological systems, the superior aerodynamic structures of birds in particular have inspired researchers in this field. In one of these studies, Bayındırlı, et al. (2020) positioned the spoiler models they developed, inspired by biological systems, in the rear section of a bus model and provided passive flow control. In this way, they achieved an improvement of up to 19% in the C_D coefficient of the bus [14]. Yanqing et al. (2023) applied grooves and protrusions on the protective helmet and examined the effects of these methods on the C_D coefficient numerically and experimentally. By protruding from the surface, the features make the laminar flow turbulent, allowing the flow to adhere to the surface more, and this delays the separation of the flow and improves the pressure-induced drag force [15].
In this study, the aerodynamic properties of a peregrine falcon bird during diving and gliding and the flow structure around the bird were examined by using CFD. Inspired by the superior aerodynamic properties of the peregrine falcon bird, passive flow control parts will be developed for aircraft and land vehicles in future studies.

2. Material and Methods

2.1. CAD design of peregrine falcon

In this study, the aerodynamic properties of the peregrine falcon were determined numerically. In the study, a 1/1 scale bird model was drawn separately for gliding and diving situations in the SolidWorks program. Bird feathers are important elements that increase their aerodynamic performance. Feathers direct airflow, reduce drag and aerodynamically optimize the bird's body. In this study, the precise structure of the feathers was drawn in a simplified manner, as it would cause mesh errors in CFD analyses. Analysis errors due to the structure of the feathers are ignored. The bird picture in nature and drawing data of the bird model in the SolidWorks® program are given in Figure 1a-b and 2a-b.

https://doi.org/10.55212/ijaa.1583570

Figure 1a. Actual drawing data of peregrine falcon at the moment of diving [9]

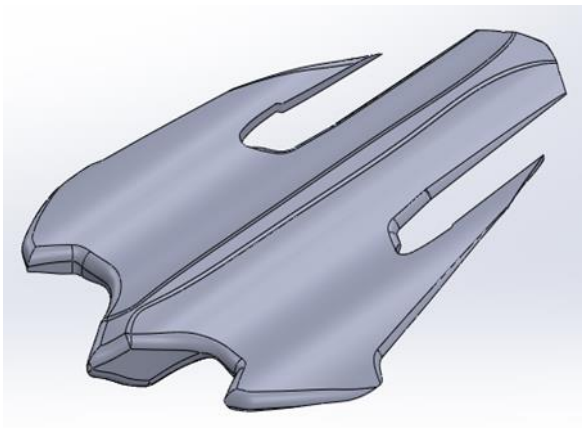

Figure 1b. CAD drawing data of peregrine falcon at the moment of diving

Figure 2a. Actual drawing data of peregrine falcon at the moment of gliding [9]

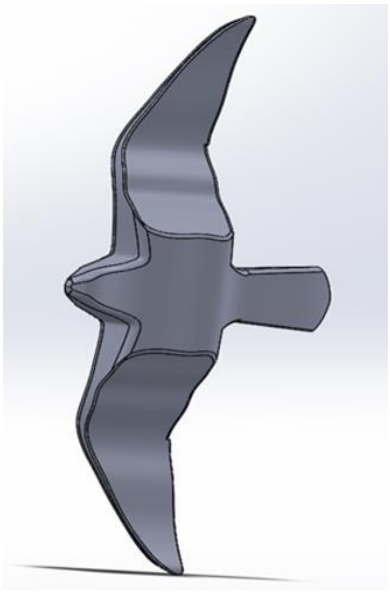

Figure 2b. CAD drawing data of peregrine falcon at the moment of gliding [9]

2.2. Providing of similarity conditions

In aerodynamic studies, three similarity conditions (geometric, kinematic, and dynamic) must be provided. The geometric similarity condition disregards minor surface irregularities. In order to ensure kinematic similarity in aerodynamic studies, the blockage rate must be lower than 7.5% [10-11]. Blockage ratio is a parameter in fluid mechanics that represents the ratio of the cross-sectional area of a model within a channel or wind tunnel to the total cross-sectional area of the channel or wind tunnel. In this study, blockage rate was lower than 10% to provide kinematic similarity. To ensure dynamic similarity Reynolds number independence was used in CFD analysis. Reynolds number is a dimensionless number in fluid mechanics that indicates whether a flow is laminar or turbulent. Reynolds number independence refers to the fact that in solving a particular flow problem, the results do not depend on the Reynolds number at sufficiently high Reynolds number values. In this case, the behavior of the flow does not change after a certain Reynolds number and therefore there is no need to increase the Reynolds

https://doi.org/10.55212/ijaa.1583570

number further when performing calculations or experiments. In short, the point is reached where the fundamental characteristics of the flow become independent of the Reynolds number.

2.3. Computational Fluid Dynamics (CFD) method

The Fluent© program used in this study solves general integral equations for continuity, momentum, energy and turbulence based on the finite volume method. During the analysis, continuity, amount of turbulence, and aerodynamic drag coefficient change graphs were monitored. The convergence of the solution was monitored from the error curves convergence graph. CFD analyses were carried out in solution domain conditions where the blocking rate was low, and the models to be analyzed were prepared in Ansys® Design Modeler, as seen in Figure 3a-b.

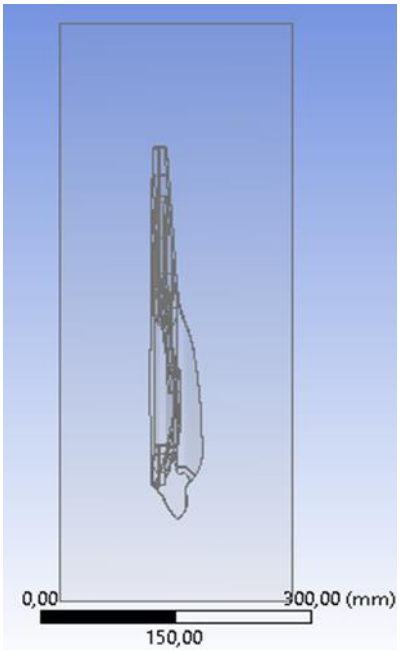

Figure 3a. Models in design modeler at the moment of diving

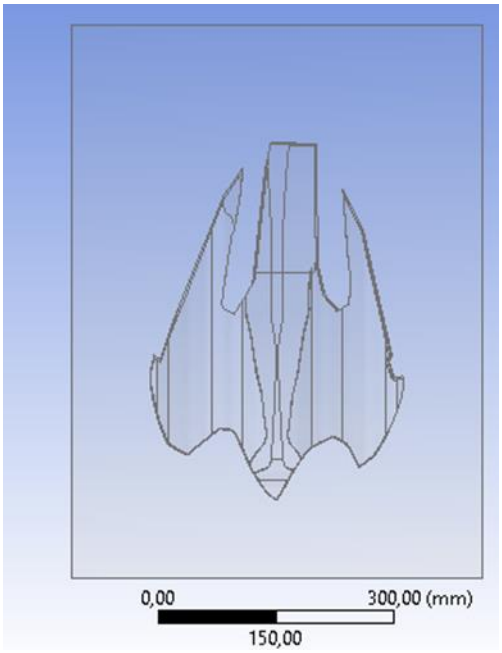

Figure 3b. Models in design modeler at the moment of gliding

Pressure and friction-induced drag forces acting on the peregrine falcon defined in the Fluent© program can be calculated separately. The total aerodynamic drag coefficient (C_D) is obtained from the sum of these two forces. Figure 4 shows the mesh structure created on the model. On the model, 2397102 triangular networks were created for gliding and 1572108 for diving moments.

The boundaries in the solution space are defined as follows. As given in Figure 5, analysis results and convergence chart were followed.

- ✓ Inlet: It is the surface where the fluid enters and is defined as the constant velocity boundary condition.
- ✓ Outlet: It is the surface from which the fluid exits and is defined as the constant pressure boundary condition.
- ✓ Wall and road (Wall): Walls are the edge surfaces of the rectangular volume that form the experimental area, and the wall boundary condition is used.
- ✓ Mold cavity (Wall) belongs to the drawing data of the model vehicle. It is the vehicle whose aerodynamic properties are determined. The wall is defined as the boundary condition.

https://doi.org/10.55212/ijaa.1583570

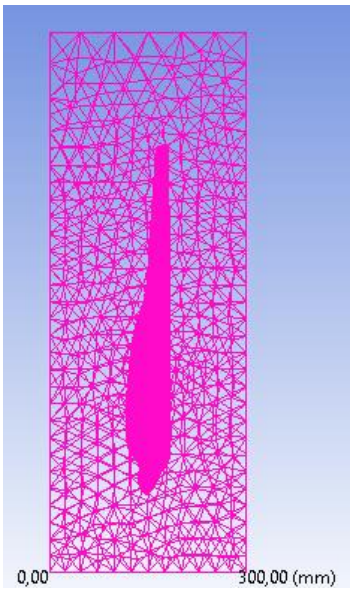

Figure 4a. Mesh distribution in CFD analysis for diving model

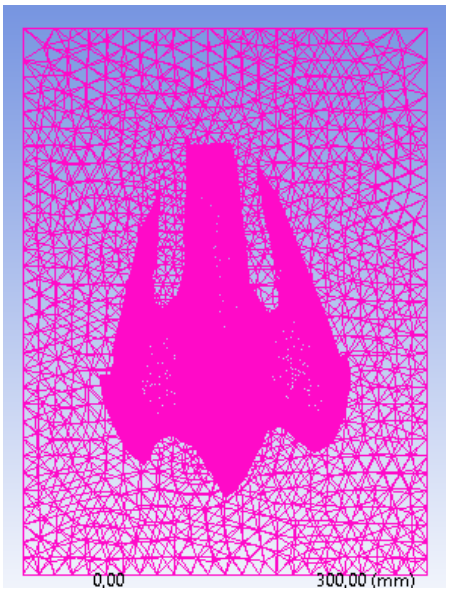

Figure 4b. Mesh distribution in CFD analysis for gliding model

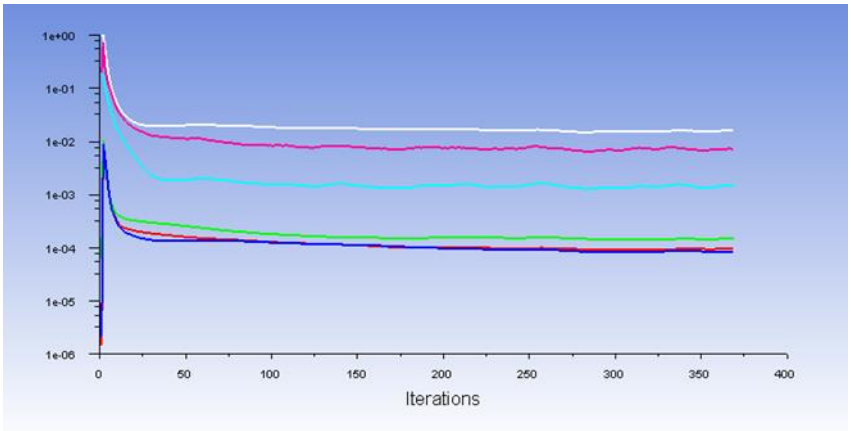

Figure 5. Convergence graph in CFD analysis

In computational fluid dynamics (CFD) analyses, air is designated as the fluid, and its properties, along with other parameters used in the analysis, are detailed in Tables 1 and 2.

Table 1. Features used in the analysis

Description	Value
Time	Constant
Velocity	Absolute
Exchange option	Node-based
Fluid	Incompressible air
Pressure – Speed connection	Simple

Table 2. Properties of the air used in the analysis

	Description	Value
ρ	Density	1 kg/m^3
μ	Dynamic viscosity	1.560×10^{-5} kg/m.s

https://doi.org/10.55212/ijaa.1583570

The aerodynamic drag coefficient (CD) is a function of the aerodynamic force (F_D), fluid density (ρ), velocity (V), and vehicle front projection area of geometry (A) as seen in Equation 1.

$$C_D = \frac{F_D}{1/2\,\rho\, V^2\, A} \tag{1}$$

Fluent© program, which is used in numerical flow analysis, solves general integral equations for continuity, momentum, energy and turbulence using the finite volume method. Continuity equation is expressed as the mass balance in the control volume in a flow, as in Equation 2.

$$\frac{\partial \rho}{\partial t} + \frac{\partial (\rho u)}{\partial x} + \frac{\partial (\rho v)}{\partial y} + \frac{\partial (\rho w)}{\partial z} = 0 \tag{2}$$

The rate of change of momentum of a piece of fluid is equal to the sum of the forces acting on this piece of fluid. The momentum increase rate of the unit volume of a piece of fluid in the x, y, and z directions is expressed by the terms, respectively. The most useful version of the Navier–Stokes equations in the finite volume method is given in Equation 3-5;

$$\rho \frac{Du}{Dt} = -\frac{\partial p}{\partial x} + div(\mu gradu) + S_{M_x} \tag{3}$$

$$\rho \frac{Dv}{Dt} = -\frac{\partial p}{\partial y} + div(\mu gradv) + S_{My} \tag{4}$$

$$\rho \frac{Dw}{Dt} = -\frac{\partial p}{\partial z} + div(\mu gradw) + S_{Mz} \tag{5}$$

3. Results and Discussion

3.1. Aerodynamic characteristics of the peregrine falcon during diving

Flow analyses were carried out at 4 different free-flow speeds. Dynamic similarity conditions were provided in all analyses. According to the analysis results, the average C_D coefficient at the time of the average dive was determined as 0.00933, and the C_L coefficient was 0.00428. The distribution of the total C_D coefficient due to pressure-friction is given in Figure 6 and Table 3. The pressure and friction distribution that creates the total drag and lift coefficients are given in Table 4.

Table 3. C_D and C_L values of results peregrine falcon while diving

Velocity (m/s)	Diving C_D	Diving C_L	Ratio of C_D/C_L
25	0.01014	0.00417	2.431
50	0.00937	0.00405	2.313
75	0.00904	0.00433	2.087
100	0.00879	0.00458	1.919
Average	**0.00934**	**0.00428**	**2.179**

https://doi.org/10.55212/ijaa.1583570

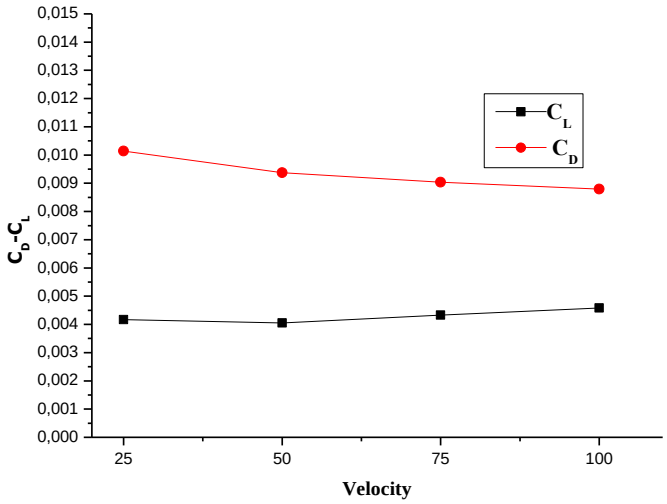

Figure 6. The graph of C_D and C_L values of peregrine falcon at the moment diving

Table 4. Pressure-friction distribution of total C_D and C_L

	Drag Force Distribution				**Lift Force Distribution**			
			Total C_D				**Total C_L**	
25 m/s	Pressure	0.0058	0.0101	57.20%	Pressure	0.0042	0.0041	99.68%
	Friction	0.00434		42.80%	Friction	~ 0		0.32%
50 m/s	Pressure	0.00572	0.0094	61.05%	Pressure	0.00404	0.004	99.75%
	Friction	0.00365		38.95%	Friction	~ 0		0.25%
75 m/s	Pressure	0.0057	0.009	63.16%	Pressure	0.0043	0.0043	99.82%
	Friction	0.0033		36.84%	Friction	~ 0		0.18%
100 m/s	Pressure	0.0057	0.0088	64.53%	Pressure	0.0046	0.0045	99.83%
	Friction	0.0031		35.47%	Friction	~ 0		0.17%

As given in Figure 7a-c, the flow structure around birds is explained by aerodynamic principles and is one of the fundamental elements enabling their ability to fly. The wings of birds have an aerodynamic profile (similar to airplane wings). The upper part is generally curved, while the lower part is flatter. The angle of the wings affects the airflow. An optimal angle of attack increases lift while minimizing drag.

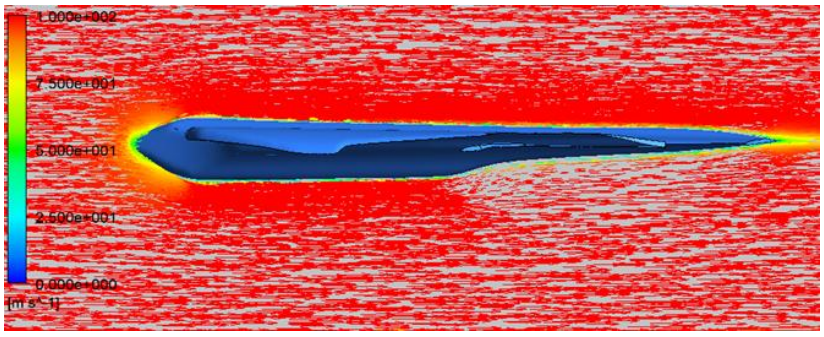

Figure 7a. Velocity vector image of the falcon bird during diving

https://doi.org/10.55212/ijaa.1583570

Figure 7b. Pressure contour image of the falcon bird during diving

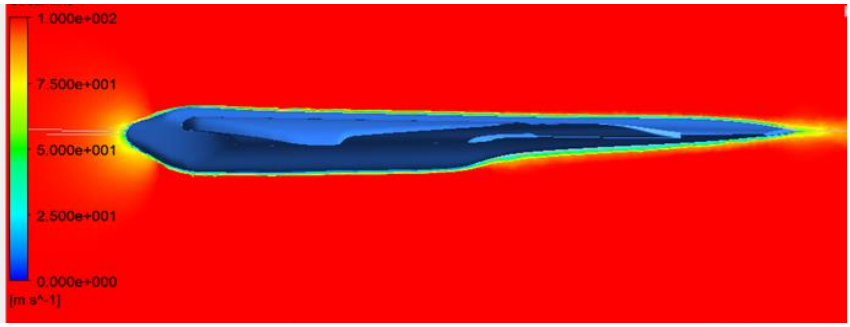

Figure 7c. Velocity streamline image of the falcon bird during diving

During a dive, the falcon folds its wings close to its body. This reduces drag, creating an aerodynamic structure and allowing it to reach high speeds. The wings form a narrow and thin profile, minimizing air resistance. This position also enhances the bird's stability. The wing and tail feathers make fine adjustments to provide steering and balance during the dive. The airflow around the bird during the dive generally remains laminar (smooth). This reduces air resistance and enables higher speeds. At high speeds or during sudden maneuvers, turbulence may occur, especially around the wing tips and tail. The falcon dynamically adjusts its body and wing position to keep turbulence under control.

3.2. Aerodynamic characteristics of the peregrine falcon during gliding

The speed of the bird when gliding is much lower than when diving. Therefore, for the aerodynamic properties of the bird to be realistic during gliding, the actual values of the bird at the moment of gliding were used as the free flow speed. CFD analyses were carried out for this model at Reynolds numbers corresponding to 10, 20, 30, and 40 m/s speeds. The C_D coefficient of the geometric shape taken by the peregrine falcon during gliding was determined as 0.02274. The average C_L coefficient was determined as 0.01653. As seen in Table 5 and Figure 8, pressure and viscous drag forces, which are among the forces that affect the drag force during gliding, progress inversely proportional to the increase in speed. As the speed increases, the pressure-induced friction force decreases and the viscous friction force also decreases.

Table 5. C_D and C_L values of results peregrine falcon while gliding

Velocity (m/s)	Gliding C_D	Gliding C_L	Ratio of C_D/C_L
10	0.02435	0.01431	1.701
20	0.02272	0.01544	1.471
30	0.0222	0.018	1.233
40	0.02169	0.01836	1.181
Average	0.02274	**0.01653**	**1.375**

https://doi.org/10.55212/ijaa.1583570

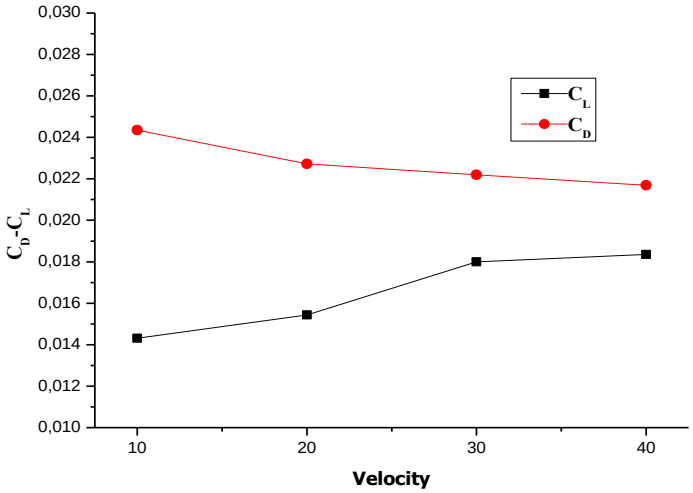

Figure 8. The graph of C_D and C_L values of a peregrine falcon at the moment gliding

Table 6. Pressure-friction distribution of total C_D and C_L

	Drag Force Distribution				**Lift Force Distribution**			
			Total C_D				**Total C_L**	
10 m/s	Pressure	0.01993	0.02435	81.85%	Pressure	0.0143	0.014309	99.94%
	Friction	0.00442		18.15%	Friction	~ 0		0.06%
20 m/s	Pressure	0.0191	0.02272	84.07%	Pressure	0.01544	0.015441	99.99%
	Friction	0.00362		15.93%	Friction	~ 0		0.01%
30 m/s	Pressure	0.0190	0.0222	85.59%	Pressure	0.0180	0.018001	99.99%
	Friction	0.0032		14.41%	Friction	~ 0		0.01%
40 m/s	Pressure	0.0187	0.02169	86.17%	Pressure	0.0184	0.018359	99.95%
	Friction	0.0030		13.83%	Friction	~ 0		0.05%

As seen in Figure 9a-c, the aerodynamic structure of a falcon during gliding allows it to conserve energy, stay airborne for long periods, and carefully observe its prey. During gliding, the falcon spreads its wings wide. This increases its wingspan, maximizing lift. The 'primary feathers' at the wingtips spread separately to control the airflow. These feathers reduce turbulence at the wingtips, minimizing energy loss. The wings are positioned at an optimal angle of attack, which increases lift while keeping drag to a minimum. The aerodynamic shape of the wings and body during gliding ensures smooth (laminar) airflow. This reduces drag and conserves energy. While small turbulences may form around the wingtips and tail, these are managed effectively thanks to the wing design. Falcons utilize gravity and thermal air currents during gliding. This relates to their ability to travel long distances without expending much energy, a flight style known as gliding flight.

https://doi.org/10.55212/ijaa.1583570

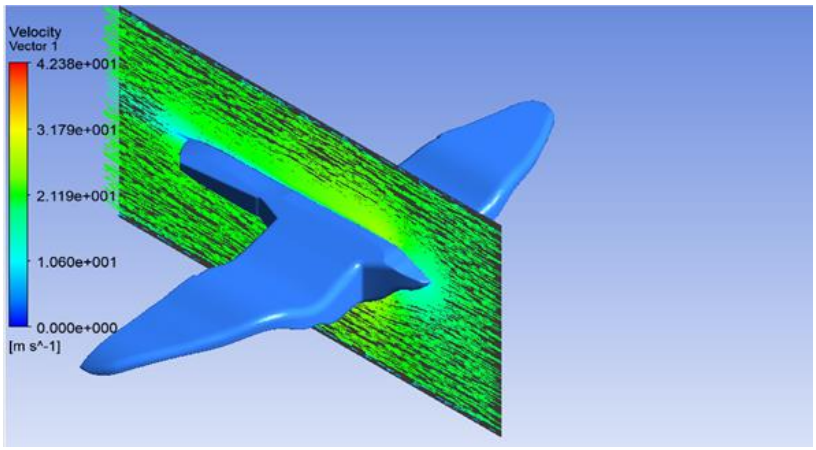

Figure 9a. Velocity vector image of the falcon bird during gliding

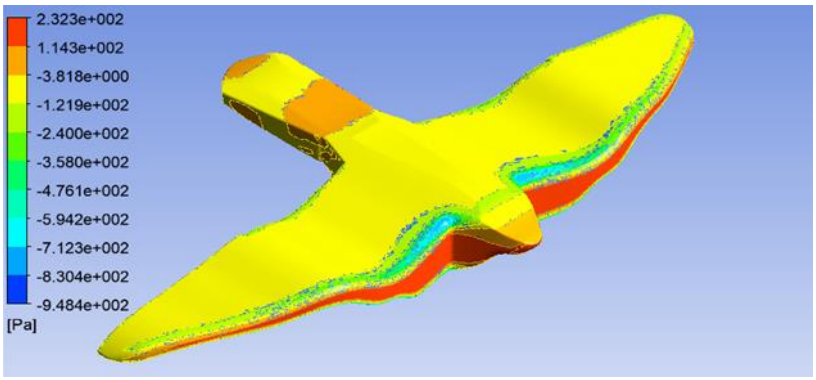

Figure 9b. Pressure contour image of the falcon bird during gliding

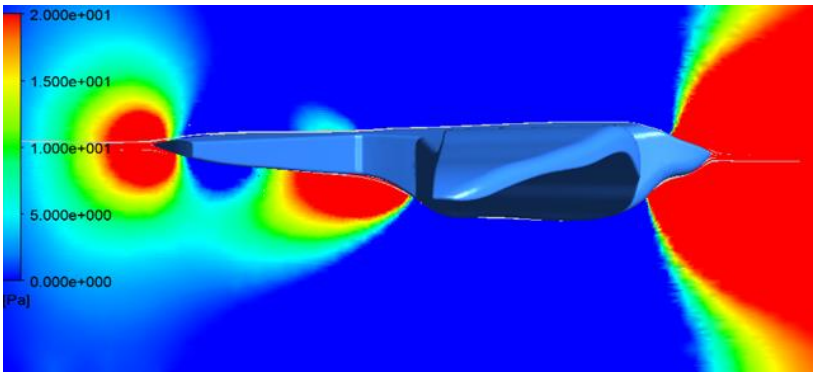

Figure 9c. Pressure streamline image of the falcon bird during gliding

The flying ability of birds is based on their perfect aerodynamic structure. This structure is important for generating lift, reducing drag, and being able to maneuver during flight. Bird wings are optimized to create lift. The upper surface of the wings is usually curved rather than flat; This increases the lift force by accelerating the airflow. The lower surface of the wings is flatter and generally more curved than the upper surface. Figure10a-b impressively explains how technology and aircraft are inspired by nature. Above is a majestic eagle in full flight, with its streamlined body and extended wings, perfectly designed for speed, agility, and efficiency in the air. Below is the famous camouflage bomber B-2 Spirit, whose design was inspired by the aerodynamics of the eagle.

https://doi.org/10.55212/ijaa.1583570

Figure 10a. Airplane models inspired by eagles [12]

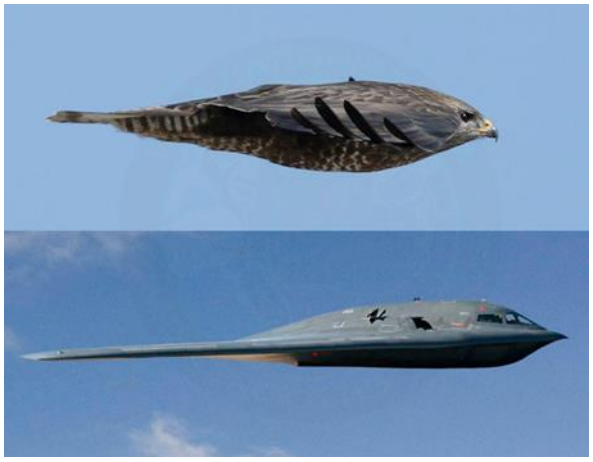

Figure 10b. Airplane models inspired by falcons [12]

Bird flight techniques have been an important source of inspiration for the aviation industry and technology development. By studying the aerodynamic principles of birds, people have developed new approaches to aircraft design and drone technologies. It has also contributed to important scientific research to understand the flight skills of birds, preserve biodiversity, and improve flight and aircraft technologies.

4. Conclusion

In this study, the aerodynamic properties of the peregrine falcon bird, the fastest animal species in nature, were examined. The geometric shape of the bird during gliding and diving was designed using CAD and flow analysis was carried out. The C_D coefficient at the moment of diving when the bird reached its highest speed was determined as 0.00934, the C_L coefficient was determined as 0.00428, and the average C_D / C_L ratio was calculated as 2.179. At the time of gliding, C_D was 0.02274, Cl was 0.01653, and the C_D / C_L ratio was determined as 1.375. While the C_D / C_L coefficient of the peregrine falcon increased by 143.6% during gliding, the C_L coefficient increased by 285.93% due to the geometric shape of the wings.

Authorship contribution statement

Cihan Bayındırlı, *Writing - original draft, Investigation, Visualization, Supervision, Conceptualization, Methodology, Software, Formal analysis.*

Conflicts of Interest: The author declares no conflict of interest.

References

[1] Ponitz, B., Schmitz, A., Fischer, D., Bleckmann, H. and Brücker, C. 2014. Diving-flight aerodynamics of a peregrine falcon (falco peregrinus). PLOS One, 9(2), e86506.

[2] Kajiwara, S. 2017. Passive variable rear-wing aerodynamics of an open-wheel racing car. Automotive Engine Technology, 2, 107–117.

[3] Smith, A. 1974. High-Lift Aerodynamics /37th Wright Brothers Lecture/. In Proceedings of the 6th Aircraft Design, Flight Test and Operations Meeting, Los Angeles, CA, USA, 12–14 August 1974, 12, 1-6. Doi.10.2514/6.1974-939.

[4] McBeath, S. 2006. Competition Car Aerodynamics: A Practical Handbook; Haynes Publishing,35-68.

https://doi.org/10.55212/ijaa.1583570

[5] Tucker, V.A. 1998. Gliding Flight: Speed and acceleration of ideal falcons during diving and pull out. Journal of Experimental Biology, 201, 403–414.

[6] https://evrimagaci.org/gokdogan-falco-peregrinus-5400 (19. September 2024)

[7] Hoyo, J., Elliott, A., Sargatal, J. and Collar, NJ. 1999. Handbook of the Birds of the World,5,14-56.

[8] Tucker, V.A., and Parrott, G.C. 1970. Bir şahin ve diğer kuşlarda süzülerek uçuşun aerodinamiği. Deneysel Biyoloji Dergisi, 52, 345–367.

[9] https://www.nationalgeographic.com/related/ca0777bc-50d1-3df7-9ff5-df8d2be22219/falcons (22 September 2024)

[10] Bayındırlı, C., and Çelik, M. 2022. Experimental Optimization of Aerodynamic Drag Coefficient Of A Minibus Model With Non-Smooth Surface Plate Application. Journal of Engineering Studies and Research, 28(4), 23-29., Doi: 10.29081/jesr.v28i3.004

[11] Çengel, Y. A. and J. M. Cimbala (2008). Fundamentals of fluid mechanics and applications. Güven Bilimsel 562-599.

[12] https://www.caneracarbay.com/2023/04/17/b-2-spiritin-hikayesi/ (20. September 2024)

[13] https://www.ansys.com/products/fluids/ansys-fluent

[14] Bayındırlı, C., Akansu, Y.E., and Çelik, 2020. Experimental and numerical studies on improvement of drag force of a bus model using different spoiler models. International Journal of Heavy Vehicle Systems, 27(6), 743-776.

[15] Yanqing, W., Ding, W., Yuju, W., Yuan. M., Lei. C., and Jiadao, W. 2023. Aerodynamic Drag Reduction on Speed Skating Helmet by Surface Structures. Applied Sciences, 2023, 13, 130, doi.org/10.3390/app1301013

https://doi.org/10.55212/ijaa.1583570